IEEE Access
Multidisciplinary ⋮ Rapid Review ⋮ Open Access Journal

Received September 30, 2020, accepted October 14, 2020, date of publication October 19, 2020, date of current version October 30, 2020.

Digital Object Identifier 10.1109/ACCESS.2020.3032203

A Method for Blind Source Separation of Multichannel Electromagnetic Radiation in the Field

SHENG LIU, BANGMIN WANG, AND LANYONG ZHANG, (Member, IEEE)
College of Automation, Harbin Engineering University, Harbin 150001, China

Corresponding author: Lanyong Zhang (zlyalf@sina.com)

This work was supported in part by the National Natural Science Foundation of China Subsidization Project under Grant 51579047, in part by the National Key Technology Support Program under Grant 2013BAG25B01, in part by the Research Fund for the Doctoral Program of Higher Education under Grant 20132304120015, in part by the Doctoral Scientific Research Foundation of Heilongjiang under Grant LBH-Q14040, in part by the National Defense Fundamental Research Funds under Grant IEP14001, in part by the Open Project Program of State Key Laboratory of Millimeter Waves under Grant K201707, and in part by the Fundamental Research Funds for the Central Universities under Grant HEUCF160414.

ABSTRACT Considering the multichannel instability, spectral overlap and strong interference of electromagnetic radiation signals in the integrated electric propulsion systems of ships, a new method is proposed which combines multivariate empirical mode decomposition (MEMD) with independent component analysis (ICA) for synchronous blind source separation of multichannel electromagnetic radiation in the field. In order to construct virtual channels, noise-aided MEMD is first applied to decompose multichannel data in this approach. Then the comprehensive screening algorithm is used to filter the intrinsic mode functions (IMFs) produced by the decomposition procedure. Finally, the new multivariate input signal is analyzed after screening using ICA to obtain the original electromagnetic radiation source signal. This method is able to effectively addresses several limitations of EMD including the mode mixing problem, its inability to handle multichannel data, as well as the indeterminacy problem in ICA. The efficacy of the MEMD-ICA algorithm was evaluated using simulated signals and real world data from a cruise ship, and comparing ensemble empirical mode decomposition-ICA(EEMD-ICA).

INDEX TERMS Blind source separation, electromagnetic environment, independent component analysis, integrated electric propulsion system, multivariable empirical mode decomposition.

I. INTRODUCTION

The integrated electric propulsion (IEP) system of a ship consists of power generators, the electrical equipment in the control room, and frequency converters/transformers. Electromagnetic radiation (EMR) is therefore most prevalent in this section of a ship. Due to space constraints, these electrical equipment are usually placed very close to each other. This can lead to intense electromagnetic interference (EMI). It is therefore necessary to perform EMR testing in IEP systems to ensure that the electrical equipment and the systems of a ship are operating normally. It is typically impossible or impractical to move this equipment to standard test sites such as electromagnetic anechoic chambers because shipboard equipment tends to be very large and require numerous auxiliary devices. Furthermore, devices that are individually EMR-compliant may exhibit incompatibilities when they are assembled into a system, which is detrimental for the operation of IEP systems. The development of on-site multi-equipment EMR testing methods for IEP systems is therefore a necessity.

The difficulty of on-site measurement is related to the filtering of the environmental background noise. The most common methods for on-site EMR testing include the use of virtual anechoic chambers [1], beamforming spatial filtering [2] and, multichannel blind source separation. Unlike single-device on-site EMR measurements where the filtering of environmental background noise is the main concern, inter-device interference between multiple devices must also be accounted for in on-site IEP system EMR measurements. In the latter, it is necessary to synchronously separate the EMR signals of multiple electronic devices with unknown electromagnetic and transmission characteristics during the filtering of the background noise. Blind source

The associate editor coordinating the review of this manuscript and approving it for publication was Huapeng Zhao.

separation (BSS) algorithms are well-suited for the separation of multichannel signals. However, due to the limitation of shipboard space, it is not possible to use a large number of antennas for EMR measurements. The BSS of IEP system signals is therefore an indeterminate problem, i.e., the number of observation signals is fewer than the number of signals sources. Consequently, the efficacy of the separation process is usually less than ideal. One possible solution to the indeterminacy problem in BSS is to add an adequate number of virtual channels via wavelet decomposition. However, this method is ill-suited to non-linear signals and it is impossible to accurately estimate the time domain features of the wavelet-decomposed signals. Furthermore, a suitable set of wavelet basis functions must be selected prior to the wavelet transform according to the features of the signals that are transformed. Thus, it is difficult to use wavelet decomposition-based methods without a priori knowledge of the signals.

Independent component analysis (ICA) is the most common method for separating independent sources without prior knowledge of the multichannel signal. However, the classic ICA algorithm is only suitable for situations where the number of input signals is larger or equal to the number of signal sources; in indeterminate cases, the results for ICA-based signal separation are usually not satisfactory [3].An important approach for resolving the indeterminacy problem in ICA is to perform ICA after the input signal is pre-decomposed to generate additional virtual channels, thus increasing the number of signals. wavelet-ICA (WICA) [4]–[7] and single-channel ICA (SCICA) [8] are some of the common methods based on this approach. WICA [9] based multiresolution analysis using a discrete wavelet transform (DWT) is shown to be more effective in removing inferences, while better preserving the structure of the source signal in both time and frequency domains However, the WICA method requires the selection of suitable wavelet basis functions according to the characteristics of the signal to be analyzed, and the wavelet decomposition is not suitable for processing non-stationary EMR signals of shipboard equipment. In contrast, empirical mode decomposition (EMD) is an adaptive data analysis method that is suitable for non-linear and non-stationary signals [10]. Compared to the wavelet transform, EMD does not require preset parameters and is easy to implement. As such, this approach is a better approach for the pre-decomposition of shipboard EMR signals. Signal processing methods based on the combination of EMD and ICA have already found widespread use in the removal of electroencephalography (EEG) artifacts [11]–[13] and fault diagnosis [14]–[16]. In [17], ensemble empirical mode decomposition (EEMD) was used to decompose multivariate data, and the intrinsic mode functions (IMFs) that contain artifactual components were screened based on the entropy and kurtosis of the IMFs. ICA was then used to extract the artifacts of the multivariate data. Finally, removal of the artifacts from the multivariate signals was achieved by performing an inverse EEMD-ICA to obtain the artifact-free multivariate dataset. Although this algorithm is widely applied in noise suppression and fault diagnosis, it is very rarely used in on-site situations for BSS of multichannel shipboard EMR signals. This is because shipboard space tends to be small, whereas EMR antennas are quite large. Thus, it is difficult to use multiple EMR antennas on a ship. EMR signal separation in ships is therefore an indeterminate BSS problem and the aforementioned algorithm is rarely used to address this problem. The indeterminate BSS problem has been discussed in [3] and [8]. In these studies, EMD was combined with ICA to solve the indeterminate BSS problem. The signal decomposition capabilities of EMD was used to expand the dimensionality of the signal, while ICA was used to separate the independent sources of the single-channel signal, thus solving the indeterminate BSS problem for single channels. Nonetheless, multivariate empirical mode decomposition (MEMD) has unique advantages compared to EMD and EEMD in the processing of multichannel signals and these advantages have been described in [18]–[21]. EMD is usually only used for single-channel signals; in the case of multichannel signals, EMD can only extract the characteristic frequencies of the IMF sets that were obtained from the independent processing of each channel. This leads to scale indeterminacy between different IMF sets and thus a lack of correlation between IMFs of the same order. It is then difficult to horizontally compare the decomposed signals. To address this problem, we propose a method for the synchronous on-site BSS of multichannel EMR signals by combining the MEMD and ICA algorithms. In our method, the indeterminate BSS problem was solved by exploiting the ability of MEMD to handle non-linear and non-stationary signals, maintain scale invariance in multi-signal decomposition, and increase signal dimensionality. This method effectively enables synchronous on-site BSS of multichannel EMR signals in IEP systems.

The novelty of the proposed MEMD-ICA algorithm is as follows:

1) Unlike artifact removal, the purpose of MEMD-ICA is to isolate signal sources from multichannel signals. It is therefore unnecessary to restore the input signals using the inverse ICA. Hence, based on the algorithmic structure of EEG artifact removal via EMD-ICA, we have proposed a novel algorithmic structure for synchronous on-site BSS of multichannel signals during shipboard EMR testing. This approach is based on the combination of the MEMD and ICA algorithms.
2) Unlike previous EMD-ICA algorithms, MEMD was introduced to ensure that the IMF sets produced by multichannel signal decomposition are correlated and scale-invariant, which is highly advantageous for the extraction of effective IMF components.
3) The proposed MEMD-ICA algorithm does not rely on noise removal preprocessing to address the noise sensitivity of MEMD. Instead, the comprehensive screening algorithm based on kurtosis and correlation are proposed. Firstly, the kurtosis interval is set to remove

noisy components from IMFs of MEMD (MIMFs), and then the correlation threshold is set to remove MIMFs that are not related to the source signals/observation signals, thus extracting IMF components containing the source signals and completing noise elimination.

The remaining portion of this paper is organized as follows. In Section II, the proposed MEMD-ICA algorithm is presented in detail, while its noise resistance and ability to handle the indeterminate BSS problem is examined through simulation experiments in Section III. Furthermore, a description of real shipboard EMR environment, the corresponding test stand, and separation results of real ship test data based on the MEMD-ICA are given and discussed in Section IV. Finally, the conclusions are drawn in Section V.

II. THE MEMD-ICA ALGORITHM

The aim of this paper is to synchronously separate the source signals from the observation signals of different channels. ICA is a better analysis method for the source separation. However, when there are fewer channels than sources, ICA by its nature cannot guarantee an efficient separation of the source signals from the observation signals and useful information may be lost [17]. Thus, it is necessary to expand the signal dimension for the decomposition of observation signals, and at the same time ensure that the signal decomposition does not affect the time-frequency characteristics of the source signals. EMD is a good method for expand the signal dimension, but the IMFs obtained for different observation channels can be different in number and properties (frequency), heavily compromising any analysis or fusion of multicomponent signals obtained in a channel-by-channel basis [21]. In addition, influenced by noise, EMD produces more irrelevant and redundant components in the decomposition process, which brings difficulties to subsequent spectral analysis and leads to repetition and aliasing [22].

To sum up, there are three problems to be solved in the combination of EMD and ICA to process multivariate data:

1) mode alignment problem.
2) Modal aliasing problem, namely similar frequencies appear across different IMFs.
3) Redundancy and Noise of EMD Decomposition Signals.

Starting from the above three problems, this paper puts forward corresponding solutions respectively. Firstly, MEMD is used to solve the asymmetry problem of IMFs sets between different variables. Then a comprehensive screening algorithm is proposed to solve the problems of signal redundancy and noise. Finally, Noise-assisted MEMD and ICA are used to solve the mode aliasing problem, and the source signals are synchronously separated from the observed signals.

A. THE DESIGN OF A NOISE-ASSISTED MEMD METHOD TO SOLVE THE MODE ALIASING AND MODE ALIGNMENT PROBLEM

In view of the complexity of the test environment, the signals received by different channels are very different. When processing multi-channel data, different channels should be guaranteed to correspond. This is reflected by the different decompositions obtained for signals with similar statistics, and the phenomenon of mode aliasing, whereby similar frequencies appear across different IMFs. The advantage of this is that the components of the channel can be analyzed by comparing the correlation between the same component and the observation channel, which is convenient for subsequent screening and processing.

MEMD has its unique advantages in processing multivariate data. Compared with EMD, MEMD shows significantly enhanced alignment of corresponding IMF from different channels in the same frequency range. The alignment of IMFs ensures that the IMF associated with the original input signal is aligned and has the same information at the same decomposition level, thus providing an intuitive and strict tool for analyzing narrow-band but non-stationary signals in real data. In addition, MEMD can overcome modal aliasing when processing complex multivariable data, so that other modals are not mixed in each IMF as much as possible. Even if the modes are aliased, the corresponding modes can be separated by subsequent ICA processing.

The standard MEMD method has been described in detail in [22] and will not be repeated here. MEMD can achieve the same characteristic frequencies in the same order of different IMF sets, which is of great significance for subsequent data integration and determination of effective components. Unfortunately, MEMD is more sensitive to noise than EMD, which will greatly limit the application of MEMD in actual signal analysis. Influenced by noise, MEMD produces more irrelevant and redundant components in the decomposition process, which brings difficulties to subsequent spectral analysis and leads to repetition and aliasing. Therefore, when MEMD is used to decompose the multivariate signals, an appropriate method is needed to solve the problems of redundancy and mode aliasing.

Herein, we propose a noise-assisted MEMD method based on EEMD listed in Algorithm 1. It should be noted that noise-assisted MEMD is not the injection of white Gaussian noise in every dimension of the multidimensional signal, but rather, the use of MEMD in the $(m+n)\times dimension$ composite space formed by noise and signals, to avoid the mode aliasing problem in MEMD.

B. COMPREHENSIVE SCREENING ALGORITHM

Although the noise-assisted MEMD method can realize multi-channel data alignment expansion and reduce the mode aliasing problem, the combination of MEMD and ICA is the core problem to be solved in this paper.

The source signals were decomposed by MEMD to produce some virtual channels. These virtual channels not only contain some white Gaussian noise, but also a large part is independent of the target source signals. Their existence not only greatly increases the computation of subsequent processing, but also affects the accuracy of separation results. Reference [23] provides an idea that the set of averaged IMFs derived from the EEMD is then applied to the FastICA

Algorithm 1 A Noise-Assisted MEMD Method Based on EEMD

Data: Dataframe df $(N \times length)$ composed of observation data of n channels
Result: Processed MIMFs
1 initialization;
2 Construct a Gaussian white noise time series $Nos(M \times length)$;
3 Combine df and Nos into a matrix $((M+N)\times length)$;
4 Use the standard MEMD algorithm to process the composite $(M+N)-channel$ signal to obtain its corresponding sets of IMF components;
5 For the $(M+N)$ IMFs that were obtained from step 3, discard the noise corresponding to the M channels;
6 the remaining IMFs of the N channels will then correspond to the signal that is being separated;

algorithm to recover the sources from the mixing matrix estimate. However, this method is not suitable for multivariate data processing. Considering that the number of MIMFs is more than the number of separation targets, if MIMFs directly use ICA, ICA will reduce the dimension according to the eigenvalue of the signal covariance matrix, which may cause MIMFs containing separation targets to be eliminated, thus causing separation failure. In addition, the number of MIMFs decomposed by multivariate data is several times that of univariate data. Considering the more sampling points of high-frequency data, this will greatly increase the computational burden. Therefore, it is necessary to perform preliminary screening and dimensionality reduction on MIMFs before ICA to avoid the loss of useful components. To sum up, this paper designs a screening algorithm that comprehensively considers the kurtosis defined in equation (1) and the correlation (equation (3)) between signals. The method first calculates the kurtosis of MIMFs to preliminarily filter Gaussian white noise, and then calculates the correlation between MIMFs and original/observed signals to further screen MIMFs. Through this screening algorithm, the original signal information can be preserved to the greatest extent while reducing the dimension of MIMFs, paving the way for subsequent ICA processing.

The kurtosis of the signal x is calculated as follows:

$$kurt = \frac{n-1}{(n-2)(n-3)}\left((n+1)\frac{m_4}{m_2^2} - 3(n-1)\right)$$
$$m_k = \frac{1}{n}\sum_{i=1}^{n}(x_i - \bar{x})^k \tag{1}$$

where n is the number of samples and $\bar{x}$ is the mean, and m_k is the $k-th$ central moment of a data sample.

The details of comprehensive screening algorithm based on kurtosis and correlation are outlined in Algorithm 2.

After MEMD processing, a BSS algorithm (i.e., ICA) is then used to perform the BSS of the EMR signal. There are two prerequisites for using ICA to perform BSS:

Algorithm 2 Comprehensive Screening Algorithm Based on Kurtosis and Correlation

input : $MIMFs$: Combination of $IMFs$ for each channel;
$S-IMFs$: By traversing the array to detect whether the index is in the interval, all non-Gaussian components are selected;
$kurtosis()$:According to equation (1), return unbiased kurtosis over requested axis;
$hist()$:Compute and draw the histogram of data;
$append()$:Append rows of other to the end of data;
$corr()$:Calculate the correlation;
$filter()$:Filter data by specified conditions;
output: $SIMFs$:Filtered IMFs

1 *Initialize MIMFs,S − IMFs,SIMFs*;
2 $kurt \leftarrow kurtosis(MIMFs)$;
3 $n, bins \leftarrow hist(kurt)$;
4 $intervals \leftarrow bins$;
5 **foreach** *the row e of MIMFs* **do**
6 **if** $kurtosis(e)$ *not in intervals* **then**
7 $S-IMFs.append(e)$;
8 **end**
9 **end**
10 By traversing the array to detect whether the index is in the interval, all non-Gaussian components are selected.
11 Calculate the correlation between $S-IMFs$ and the source signals/observation signals.
12 **foreach** *the row e of* $S-IMFs$ **do**
13 **if** $corr(e,S) > threshold$ *and* $n > numbers$ **then**
14 $eIMFs \leftarrow filter(S-IMFs)$;
15 $SIMFs.append(eIMFs)$;
16 **end**
17 **end**
18 perform deduplication and remove components with low correlation.

1) The source signals must be statistically independent.
2) The source signals cannot be Gaussian signals [11].

While the EMR signals of the shipboard signal sources are emitted by different equipment, each of these signals will exhibit the intrinsic EMR of each equipment. The distribution of the source signals is difficult to determine in advance, and if the assumed distribution of the traditional ICA algorithm is far from the real distribution, it may lead to poor performance. This requires an ICA algorithm that can deal with a wide range of distributions. The ICA algorithm used in this work is the ICA-EBM [24], where the maximum entropy bound is used to approximate the entropy given the observations. By using a few simple measuring functions, a tight entropy bound can be determined for sources that come from a wide range of distributions. In addition, compared to traditional ICA, ICA-EBM is more attractive due to its superior separation performance,reliable convergence, moderate computational complexity and high flexibility of density matching.

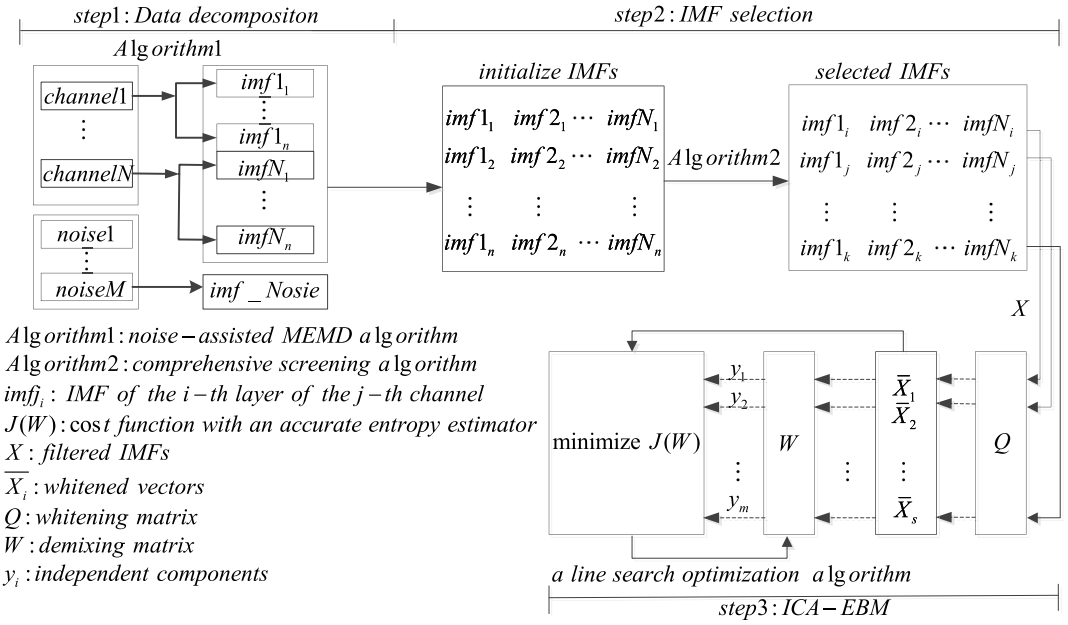

FIGURE 1. Block diagram of the structure of the MEMD-ICA algorithm.

ICA-EBM may therefore be used to separate the signals of the IEP systems.

C. THE IMPLEMENTATION OF THE MEMD-ICA METHOD

A block diagram of the algorithmic structure of MEMD-ICA is shown in Figure 1. This algorithm may be divided into three steps:

1) The signal with N channels that was acquired by the sensors is decomposed via MEMD into N sets of IMFs of equal length.
2) The IMFs are re-ordered, and Algorithm 2 is performed. Herein, a kurtosis interval is defined to discard the noise component, and correlation threshold is set to remove irrelevant components.
3) The selected IMF sets are organized to form a new input signal, X, which is first processed using principal component analysis (PCA) to reduce the dimensionality of the raw data, thus yielding a dimension-reduced signal, $\overline{X}$. This signal is then passed to the ICA-EBM algorithm to separate the Y signals from the M inputs.

The details of the MEMD-ICA algorithm are described in Algorithm 3.

To evaluate the performance of the proposed approach, MEMD-ICA was tested against EEMD-ICA. Three batches of experiments on the source separation were performed using simulated data and real world data from a cruise ship, respectively. It is necessary to compare MEMD-ICA and EEMD-ICA theoretically before the simulation test, which will be helpful to the analysis of the test results. Comparing with MEMD, EEMD has significant shortcomings as follows:

1) `Nonuniformity`: EEMD is not likely to yield the same number of IMFs for every data channel.
2) `Scale alignment`: There is no guarantee that same-index IMFs would contain equal scales across data channels, and variations among distinct channels would inevitably result in differences in the extracted IMFs.
3) `Nature of IMFs`: Enforcing the same number of IMFs for every data channel may compromise time-frequency(TF) estimation, as such IMFs are typically not monocomponent.
4) `Computational complexity`: EEMD is a major algorithm to robustly perform EMD, at a cost of increased computational complexity [18].

Algorithm 3 The MEMD-ICA Algorithm

Data: Dataframe df $(N \times length)$ composed of observation data of n channels
Result: the estimated source signals $\hat{S}$

```
Initialize ICA-EBM: measuring function G(x) = x^4,
maximum number of iterations
max_iter = 100,threshold value tol = 0.001,number of
components to use n_components;
Perform Algorithm 1;
Set kurt interval and corr threshold;
repeat
    Execute comprehensive screening algorithm listed in
    Algorithm 2 ;
    Discard noise and uncorrelated components;
until Number of elements in SIMFs = >n_components;
Construct new multivariate signal X;
Perform a standard preprocessing procedure;
Calculate ICs via ICA-EBM;
```

III. SIMULATION VALIDATION

In this section, the noise resistance of the MEMD-ICA algorithm and its ability to handle the indeterminate BSS problem is examined through simulation experiments. An approach

upon ensemble empirical mode decomposition and ICA algorithm(EEMD-ICA), which serves as a comparison for the evaluation of the MEMD-ICA algorithm, has been described in [17]. When processing multi-channel observation signals, EEMD-ICA algorithm decomposes single-channel observation signals into a set of noise-canceled intrinsic mode functions, which are sequentially separated by ICA-EBM algorithm. The simulation validation of our proposed algorithm involves two aspects:

1) Efficacy of the algorithm with the introduction of noise.
2) Validation of the algorithm's efficacy in handling the indeterminate BSS problem, i.e., the number of signal sources is greater than the number of input signals.

After the MEMD-ICA algorithm realizes the separation of multiple mixed signals, mean square error (MSE) and cross-correlation coefficient (CRC) were regarded as the assessment criteria to quantitatively evaluate the performance of proposed method.

If $\hat{s}_i$ is the predicted signal value of the $i-th$ sample, and s_i is the corresponding true value, then the mean squared error (MSE) estimated over n_{samples} is defined as

$$\text{MSE}(s, \hat{s}) = \frac{1}{n_{\text{samples}}} \sum_{i=0}^{n_{\text{samples}}-1} \left(s_i - \hat{s}_i\right)^2 \tag{2}$$

The CRC between two signals is calculated as follows:

$$CRC = \frac{\sum (x - m_x)\left(y - m_y\right)}{\sqrt{\sum (x - m_x)^2 \sum \left(y - m_y\right)^2}} \tag{3}$$

where m_x is the mean of the signal x and m_y is the mean of the signal y.

Among them, MSE represents the accuracy of signal separation, and CRC measures the structural similarity and indicates the degree of covariance between the separated signal and the original signal. Considering that the ICA separation results are inconsistent with the original signals in amplitude, it is necessary to standardize the signals before measuring the separation results.

A. SIMULATION VALIDATION 1

Simulation experiments verify the effectiveness of the proposed algorithm from two aspects respectively. First, MSE and CRC are used as indexes to verify the separation of different types of signals by MEMD-ICA under different signal-to-noise ratios. Secondly, by adding new source siganl type, the number of observation channels is smaller than the number of original signals to simulate the problem of underdetermined blind source separation, and the blind source separation capability of MEMD-ICA under underdetermined conditions is tested.

In order to ensure that the simulation experiment is as close to the complex and changeable actual environment as possible, this paper improves the scheme that the existing literature uses a single type of signal with different frequencies as the original signal, and introduces different types of signals as the original signal. The original signals used in this part

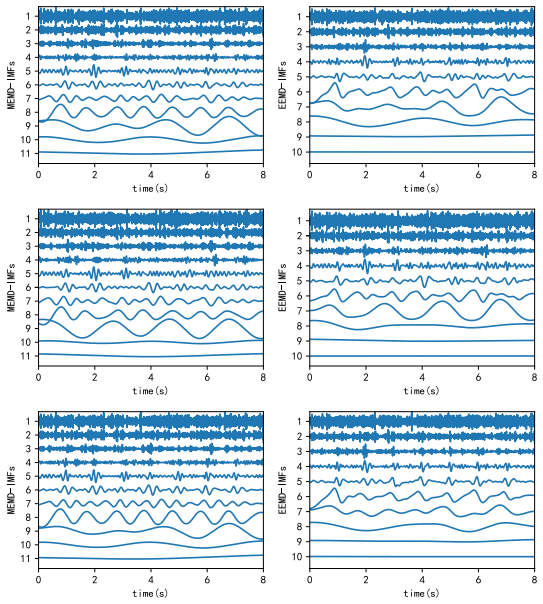

FIGURE 2. Left: decomposed MIMFs, when the MEMD algorithm is supplied with the observation signal0(top),signal1(middle), and signal2(bottom). Right: decomposed EIMFs using the EEMD method with the same signals.

of simulation include sinusoidal signal, square wave signal and sawtooth wave signal. In addition, EEMD-ICA is used as a comparison algorithm to verify the effectiveness of the proposed MEMD-ICA algorithm.

sinusoidal signal, square wave signal and sawtooth wave signal were configured as follows:

$$\begin{aligned} s_1 &= sin(2t) \\ s_2 &= sign(sin(3t)) \\ s_3 &= sawtooth(2\pi t) \end{aligned} \tag{4}$$

The parameters of this signal are as follows: t is a time series determined by the number of sampling points $N = 2000$ and sampling frequency $f_s = 125\ Hz$. The $sign$ function returns -1 if $x < 0$, 0 if $x == 0$, 1 if $x > 0$. The sawtooth waveform has a period 2π, rises from -1 to 1 on the interval 0 to $width * 2\pi$, then drops from 1 to -1 on the interval $width * 2\pi$ to 2π. $width$ must be in the interval [0, 1].

In addition, in order to verify the characteristics of the proposed algorithm under different signal-to-noise ratio(SNR),the data of SNR was set from 0.1 to 1.5. For each type of signal, 50 random interferences at each SNR level are projected to 50 ''clean'' epochs of various types of signals. The average MSE of 50 simulation tests was calculated. Afterwards, according to the mixing matrix A, the observed signals $x1$, $x2$, $x3$ are obtained by linearly combining the noise superimposed $s1$, $s2$, $s3$, where the mixing matrix A is as follows:

$$A = \begin{bmatrix} 1 & 1 & 1 \\ 0.5 & 2 & 1 \\ 1.5 & 1 & 2 \end{bmatrix} \tag{5}$$

Figure 2 shows the decomposition results of MEMD algorithm and EEMD in time domain, respectively. It is worth

TABLE 1. Key parameters of EEMD-ICA and MEMD-ICA methods.

	kurt interval	corr threshold	ICA-EBM		
			G(x)	max_iter	tol
EEMD-ICA	[-0.171,0.216)	0.3	x^4	200	0.001
MEMD-ICA	[-0.011, 0.351)	0.3	x^4	200	0.001

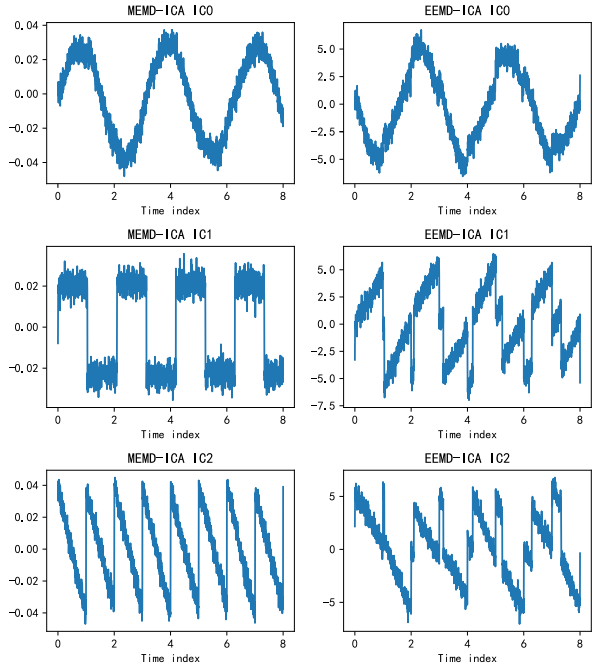

FIGURE 3. Decomposition results of MEMD-ICA and EEMD-ICA under $SNR = 1.5$.

noting that the multivariate signal has the same number of decomposition levels after MEMD decomposition, which is determined by the algorithm characteristics of MEMD, while EEMD is difficult to ensure the consistency of the decomposition number of each channel because it decomposes each channel independently. In addition, it can be seen from MIMF9 that IMF of the same order has the same characteristic frequency, while EEMD does not have this characteristic, which is one of the advantages of MEMD over EEMD in processing multiple input signals. This characteristic is useful for the retrieval of source signal-containing IMFs, because the same set of MIMFs have the similar characteristic frequency, the selection efficiency can be improved when IMFs component selection is carried out. In terms of modal aliasing, MEMD decomposition can already see the single frequency characteristics of signals in MIMF9, which shows that MEMD has performed well compared with EEMD in processing multivariate signals although there is still a certain degree of modal aliasing.

After that, the IMFs are screened according to Algorithm 2, and the key parameters used in EEMD-ICA and MEMD-ICA are listed in Table 1. The decomposition results of MEMD-ICA and EEMD-ICA under $SNR = 1.5$ are shown in Figure 3. By comparing MEMD-ICA with EEMD-ICA, it may be observed that MEMD-ICA decomposition can solve the mode aliasing problem caused by using MEMD decomposition alone. It is qualitatively proved that MEMD-ICA algorithm is more suitable for blind source separation of multi-type noisy signals than EEMD-ICA.

In addition, Frequency spectra mixing tends to occur when MEMD is used to decompose multivariate signals because the MEMD algorithm is sensitive to noise [22]. Therefore, noise reduction preprocessing is necessary when MEMD is used to process multivariate signals. However, since kurtosis and correlation-based filtering and ICA-EBM post-processing were incorporated in the proposed MEMD-ICA algorithm, this algorithm can be used to separate signal sources without noise reduction preprocessing. This is also one of the major advantages of the proposed algorithm.

The above qualitatively compares the two algorithms in dealing with the problem of multi-type noisy blind source separation. Next, we will quantitatively separate the changes of performance indexes of the two algorithms under different SNR. MSE and CRC of MEMD-ICA and EEMD-ICA separation results with original signals under different SNR are shown in Figure 4. First of all, from the index NMSE, when the SNR is low, the separation effect of MEMD-ICA and EEMD-ICA is similar, but with the increase of SNR, the NMSE of MEMD-ICA decomposition results decreases faster and is always smaller than that of EEMD-ICA. Although the changes of different types of signals are different, the general trend of the three types of signals is the same. Then, we compare the CRC index of the two algorithms. First of all, the CRC index of the two algorithms is increasing with the increase of signal-to-noise ratio, and the CRC index of MEMD-ICA is always better than that of EEMD-ICA. From the point of view of signal type, MEMD-ICA has greater advantages than EEMD-ICA in separating square wave signals.

To sum up, the separation effect of MEMD-ICA is better than that of EEMD-ICA both qualitatively and quantitatively, and MEMD-ICA has its own unique advantages in processing some special signals such as square wave signals.

B. SIMULATION VALIDATION 2

To verify the effectiveness of the proposed MEMD-ICA algorithm in handling the indeterminate BSS problem, A Frequency-swept cosine generator is added to the source signals of simulation verification 1 to generate a chirp signal as a new source signal, which was configured as follows:

$$s_4 = chirp(t, f0, f1, t1, method = \text{“}linear\text{”}) \tag{6}$$

The parameters of this signal are as follows: f_0 =6 Hz, f_1 =1 Hz, t_1 = 8s, t is a time series determined by the number of sampling points N = 2000 and sampling frequency $f_s = 125\ Hz$. Where $f0$ and $f1$ represent frequencies (e.g. Hz) of the generated signal at 0 and $t1$, respectively. The $method = \text{“}linear\text{”}$(e.g. $f(t) = f0 + (f1 - f0) * t/t1$) gives the instantaneous frequency (in Hz) of the signal generated by *chirp*().

Based on the configuration of the simulated signal, the observation signals x_1, x_2, x_3 are linear combinations of four signal sources, where the mixing matrix A was

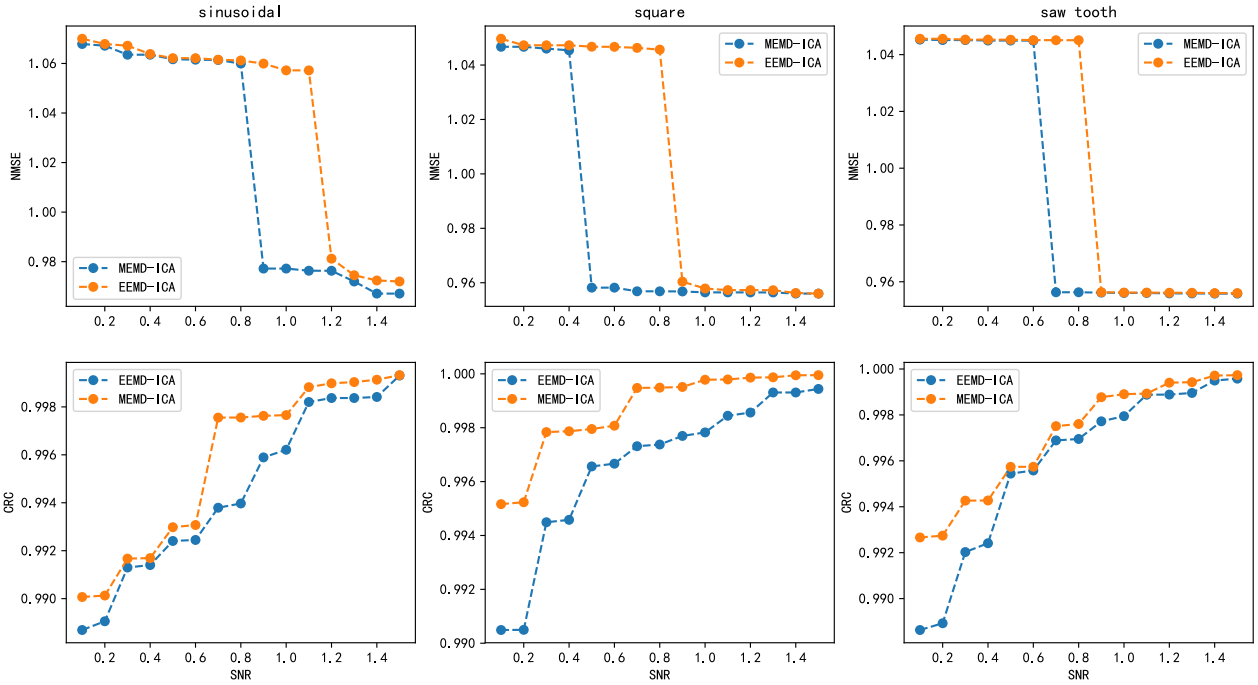

FIGURE 4. MSE and CRC of MEMD-ICA and EEMD-ICA separation results with original signals under different SNR.

TABLE 2. Key parameters of EEMD-ICA and MEMD-ICA methods.

	kurt interval	corr threshold	ICA-EBM		
			G(x)	max_iter	tol
EEMD-ICA	[-1.386,0.680)	0.3	x^4	200	0.001
MEMD-ICA	[-0.041, 0.103)	0.3	x^4	200	0.001

configured as follows:

$$A = \begin{bmatrix} 1 & 1 & 1 & 1 \\ 0.5 & 2 & 1 & 1 \\ 1.5 & 1 & 2 & 1 \end{bmatrix} \tag{7}$$

If ICA-EBM is directly used to process this signal, four signal sources have to be separated from three input signals. This is therefore an indeterminate problem and it is difficult to obtain ideally separated signals using ICA alone. According to the proposed MEMD-ICA algorithm, the first step of the algorithm is to complete MEMD decomposition of the simulated signals. Next, the kurtosis and correlation for each component are calculated. After the first four sets of IMFs were combined to form a new multivariate input signal. The new input signal was then processed using the ICA-EBM algorithm. the key parameters used in EEMD-ICA and MEMD-ICA are listed in Table 2.

Different from the simulation verification 1, this part simulates the underdetermined blind source separation problem by adding new noise types to make the number of observation channels smaller than the original signal number, and tests the blind source separation capability of MEMD-ICA under underdetermined conditions. Similarly, this section also uses MEMD-ICA and EEMD-ICA to process the same signal respectively, so the process results will not be discussed again here. This part only analyzes the final separation results, and CRC and MSE are still used as measurement indexes for the two algorithms. The results are shown in Figure 5.

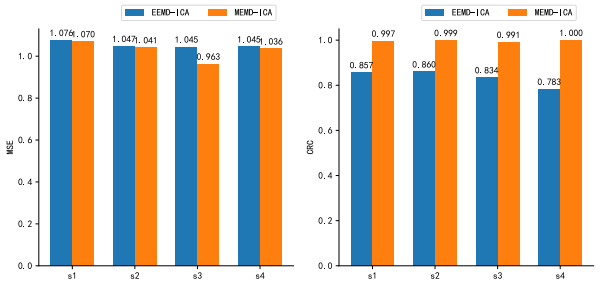

FIGURE 5. Measurement indexes for the MEMD-ICA and EEMD-ICA algorithms.

As far as MSE index is concerned, in general, that MSE of the MEMD-ICA separation result and the original signal of each channel are always lower than that of the EEMD-ICA separation result, but they are still very close, except that the MSE of the MEMD-ICA for $s3$ is lower. This shows that MEMD-ICA has more advantages than EEMD-ICA in dealing with sawtooth waves. In contrast, the correlation between MEMD-ICA and EEMD-ICA is higher than that of EEMD-ICA in terms of CRC index, and even the correlation between EEMD-at $s4$ is lower than 0.8, which indicates that the decomposition of $s4$ by EEMD-ICA has been seriously deformed. No matter from which index, MEMD-ICA is more suitable than EEMD-ICA to deal with underdetermined blind source separation.

Similarly, this part also compares the separation effects of the two methods from a qualitative point of view, as shown in Figure 6. It can be seen from the figure that the $s3$ separated by EEMD-ICA has been seriously deformed, which is consistent with the results of quantitative analysis. On the other hand, the separated $s3$ of MEMD-ICA is also

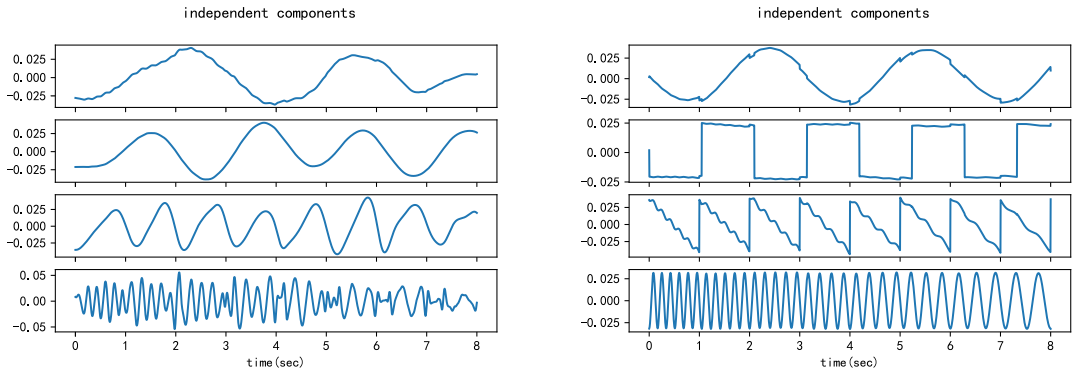

(a) Results of EEMD-ICA separation in indeterminate conditions.

(b) Results of MEMD-ICA separation in indeterminate conditions.

FIGURE 6. Instantaneous spectrum of the MIMFs and EIMFs components of channel 0.

consistent with the quantitative analysis result, which basically coincides perfectly with the $s3$ of the original signal. This shows that MEMD-ICA is very suitable for processing time-varying signals, which is also consistent with the application environment in this paper.

To sum up, MEMD-ICA has better performance than EEMD-ICA in dealing with underdetermined blind source separation. Of course, the conditions set by the simulation test are relatively simple after all, which is far from being compared with the complex electromagnetic environment in the actual test environment. Therefore, it is necessary to verify the processing effect of MEMD-ICA on the actual test signal in the next part.

IV. PRACTICAL VALIDATION IN AN ACTUAL SHIP

After validating the MEMD-ICA algorithm in simulations, it was necessary to validate the algorithm in a practical environment (i.e., in a ship) since the simulation validation only provides theoretical proof of the algorithm's utility. Real shipboard EMR environments are much more complex and subject to interference due to a variety of sources of noise. In this section, the proposed MEMD-ICA algorithm will be used to process the data acquired from actual ship measurements, to prove the efficacy of the algorithm in practical applications.

The tests were performed on the propulsion system of a cruise ship as shown in Figure 7. EMR data was collected from its generators, control room switchboards and frequency converters. The system that was used to record the EMR measurements is shown in Figure 8. The measurement system contained three embedded NI PXIe-5624R digitizers, and the EMR signals were acquired using three measurement antennas. In this figure, it is shown that there are many sources of EMR in the shipboard environment. The signals from equipment in this space are most likely coupled with each other, and it is difficult to obtain a priori knowledge on their EMR characteristics. Furthermore, it is very likely that the antennas will be subjected to environmental noise during the operations of the cruise ship. Therefore, the testing environment in cruise ships is a classic blind multichannel source separation problem.

FIGURE 7. The cruise ship where the actual ship tests were conducted.

FIGURE 8. Photograph of a testing site inside the cruise ship.

Figure 8 also shows that three antennas were used in the EMR measurement system. The reason for this is because:

1) It was not possible to use more antennas due to space limitations.
2) Three antennas provide sufficient information on the EMR of the electrical equipment. One of the advantages of the proposed algorithm is its ability to separate the EMR signals emitted by several

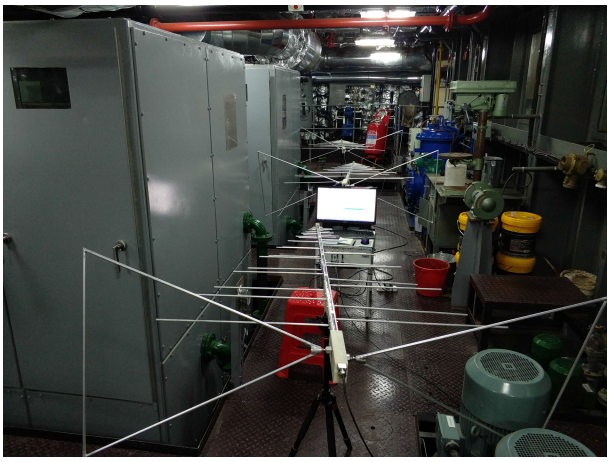

FIGURE 9. Measurement of the EMR signals from four generators that were operated at their rated condition.

equipment using a relatively small number of hardware devices.

The EMR data measured from four actual ship generators were used to validate the efficacy of the proposed MEMD-ICA algorithm. The conditions were selected to ensure that there were four well-defined signal sources. As a comparison method, to verify the validity of the proposed algoritm, the EEMD-ICA will also process the same signals synchronously. Furthermore, the requirements of this experiment for high levels of noise interference and indeterminacy were fulfilled by the intense environmental noise that is always present in the generator cabin. The sampling parameters were configured as follows: sampling frequency $f_s = 2GSa/s$, memory depth $N = 4M$, sampling time $t = \frac{N}{f_s} = \frac{4\times10^9}{2\times10^9}s = 2ms$. The measurements were performed when the cruise ship was operating at its rated condition. The layout of the measurement system and its antennas is illustrated in Figure 9. The gap between the antennas was 2.5 m, and each antenna was placed at a height of 1.5 m. The three antennas were arranged in a straight line.

Figure 10(a) respectively show the magnitude spectrum of the EMR signals acquired using Antenna 1,2,3 and the coherence between channels. By comparing the EMR signals that were obtained from the three antennas, it was determined that the EMR signals produced by the generators at their rated condition cover a broad range of frequencies, and the EMR signals obtained by each antenna differ significantly from each other. From the coherence between channels, it can be seen that the common components between signals of each channel are roughly understood, and the frequency points with coherence above 0.8 are collected in Figure 10(b). This result is caused by couplings between the EMR signals of the four generators. The proposed MEMD-ICA algorithm was then used to separate the EMR signals of each generator from the mixed EMR signals that were collected by the three aforementioned antennas (channels).

According to the proposed algorithm and EEMD-ICA, MEMD decomposition and EEMD were respectively applied to the mixed EMR signals that were collected via three

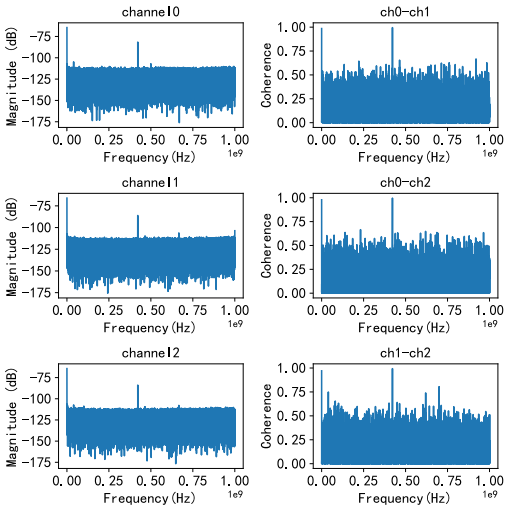

(a) Magnitude spectrum of the EMR signals for each channel and coherence between Channels.

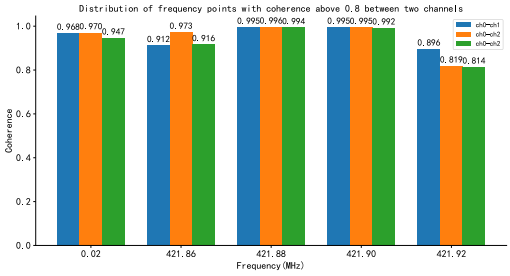

(b) Distribution of frequency points with coherence above 0.8 between two channels.

FIGURE 10. The magnitude spectrum of the observation channel, the coherence between the two and the key frequency points.

observation channels(OCs). The results are shown in Figure 11. In this figure, it is shown that the actual signals are mixed with multifrequency source signals; consequently, the decomposition levels of the MEMD algorithm are much more complex in this case compared to the simulation validations. Nonetheless, a vertical comparison reveals that comparing with EIMFs, MIMFs still have similar time domain waveforms. Hence, the MIMFs of the same order generally contain the same information about the frequencies of the source signals. Furthermore, this paper calculates the instantaneous frequencies of MIMF9-15 and EIMFs components of channel0 respectively, as shown in Figure 12. From the figure, it can be found that the decomposition results of the last layers of MEMD no longer have instantaneous frequencies, while the corresponding parts of EEMD still contain more instantaneous frequencies.Therefore, compared with EEMD, MEMD has more advantages in dealing with complex and changeable signals.

Next, according to the proposed algorithm, the kurtosis is calculated and the distribution histogram is drawn in Figure 13 to eliminate the Gaussian component. It is noteworthy that the kurtosis 0 corresponds to the Gauss distribution. Components far from the Gauss distribution contain more source signal information. Afterwards, the correlation

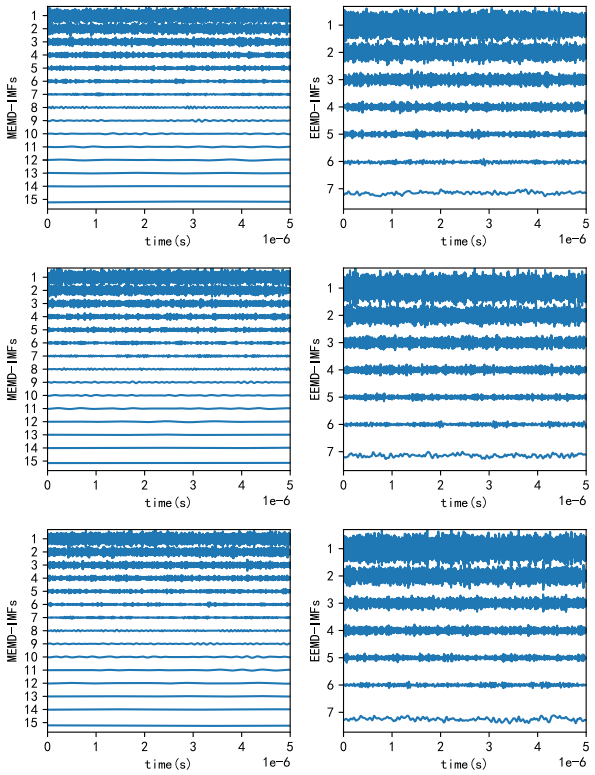

FIGURE 11. Left: decomposed MIMFs, when the MEMD algorithm is supplied with the observation channel0(top),channel1(middle), and channel2(bottom). Right: decomposed EIMFs using the EEMD method with the same channels.

between the remaining components and the observation channels is calculated, and the distribution histogram is drawn in Figure 14.

According to a preset threshold, the proposed algorithm eliminates the components with low correlation. With this, the Gaussian noise in the MIMFs and the EIMFs and the components independent of the original signal are all filtered out. Subsequently, they form a new input signal matrix for subsequent ICA-EBM. Here, the parameters of the ICA-EBM are consistent with Table 2. After completing the above steps, the proposed algorithm realizes the separation of the observation signals of the four generator sets, and the spectrum of the separation results is shown in Figure 15.

Considering that the EMR signals of the generator set itself can not be obtained in the field test environment, it is impossible to directly calculate MSE and CRC of the original signal between ICs as performance evaluation indexes. this paper intends to prove the effectiveness of the proposed algorithm from three aspects:

1) Compare the performance indexes of MEMD-ICA and EEMD-ICA.
2) Qualitative analysis of the relationship between ICs and key frequency points of observation channels(Figure 10).
3) Compare the correlation of time and frequency domain between ICs channels.

Firstly, Considering that each source signal is a component of the observation signals, so ICs must have a

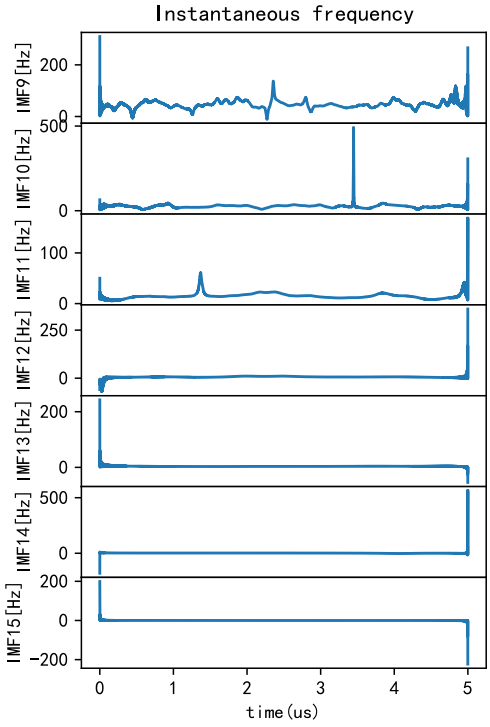

(a) Instantaneous Spectrum of MIMF9-15 for Channel 0

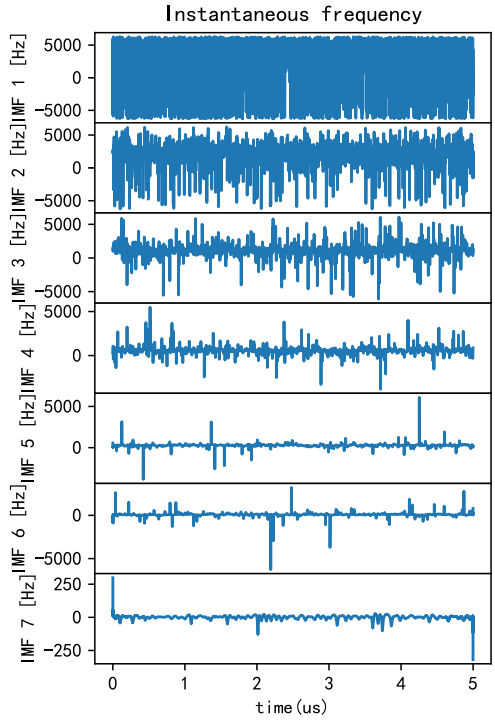

(b) Instantaneous Spectrum of EIMFs for Channel 0

FIGURE 12. Instantaneous spectrum of the MIMFs and EIMFs components of channel 0.

high correlation with the observation signals. Of course, because there are other components in the observation signal, their correlation will not be too high, but it is sufficient as an evaluation index. Based on the above analysis, We drew separately correlation between MEMD-ICA

TABLE 3. Comparison of EEMD-ICA and MEMD-ICA methods.

	IMFs	Correlation (IMFs and OCs)			S-IMFs	Correlation(ICs and OCs)			kurt interval	corr threshold	wall time
		s1	s2	s3		s1	s2	s3			
EEMD-ICA	21	0.7127	0.7237	0.7189	6	0.7352	0.5567	0.5602	[-0.056,0.219)	0.4	1min 39s
MEMD-ICA	45	0.7571	0.7562	0.7575	7	0.7742	0.7725	0.7093	[-0.042,0.081)	0.4	46s

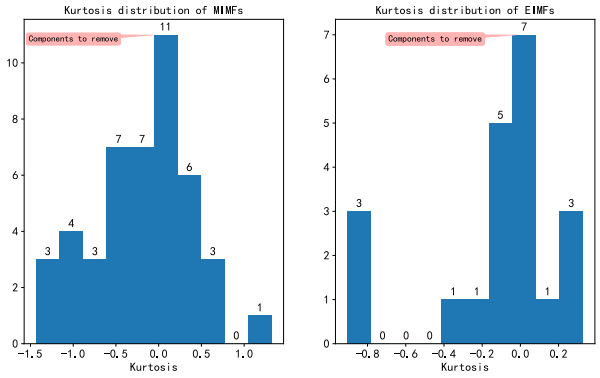

FIGURE 13. Kurtosis distribution of MIMFs and EIMFs components.

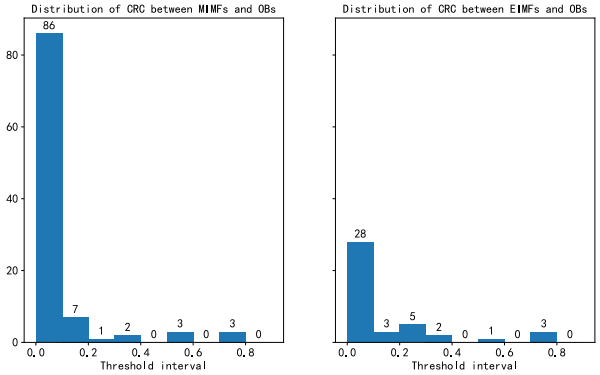

FIGURE 14. Comparison of correlation coefficient distribution between MIMFs, EIMFs, and observation channels.

and EEMD-ICA separation results and OCs under different thresholds, as shown in Figure 16. Comparing the decomposition results of EEMD-ICA and MEMD-ICA horizontally, the correlation between the decomposition results and each observation channel is higher, which proves the advantages of the proposed algorithm over the existing algorithms. From the decomposition results of MEMD-ICA itself, the IMFs begin to decrease with the increase of the threshold, and the correlation between the decomposition results of MEMD-ICA and the original channel gradually increases, which proves that the accuracy of the decomposition results is effectively improved through comprehensive screening algorithm. As a summary, Table3 shows the separation performances and process parameters for The EMR data measured from four actual ship generators using MEMD-ICA, and EEMD-ICA methods,where the MIMFs and EIMFs were selected based on Figure 13 and 14 and the selection of threshold. It is worth noting that comparing the wall time of the two algorithms, we can see that EEMD-ICA has higher computational complexity.

Secondly, from the angel of qualitative analysis, the separation results in Figure 15 include the key coherent

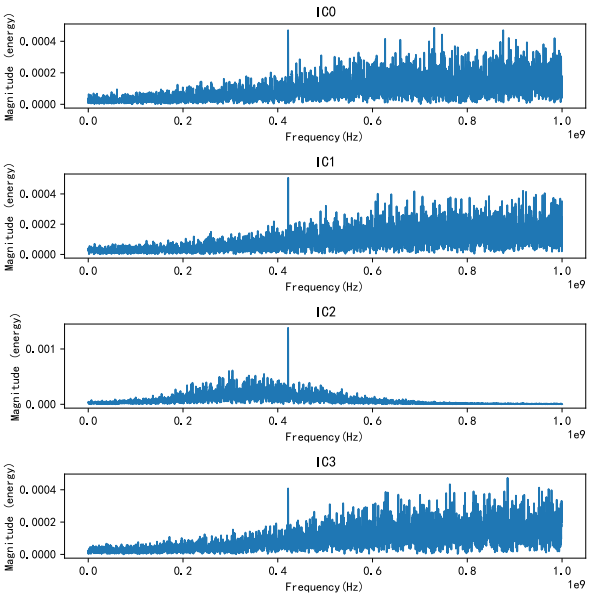

FIGURE 15. Frequency-domain waveforms of the EMR of each generator.

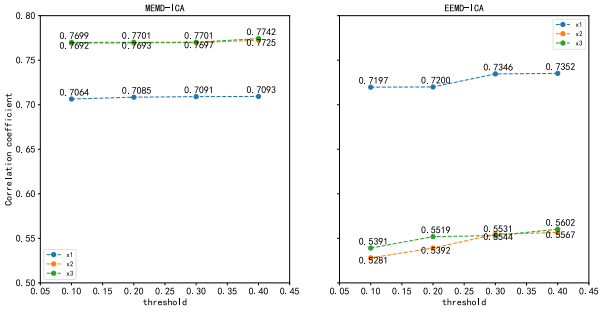

FIGURE 16. Correlation between MEMD-ICA and EEMD-ICA separation results and observation channels under different thresholds.

frequency (Figure 10 (b)) points of the observed signals. which proves that the separation results are all related to the source signals.

Third, the correlation coefficient of the separation results is calculated and the results are plotted as Heatmap(Figure17). The correlation coefficients of different *ICi* in the figure are very low(approximately 10^{-6}), which proves that different ICs are irrelative in time domain. Furthermore, as shown in Figure18, it can be seen that although there is correlation between ICs at individual frequencies, the maximum value of correlation is below 0.5, indicating that ICs are not correlated with each other in the frequency domain. Thus, it is proved that the ICs are uncorrelated in both time domain and frequency domain.

To sum up, ICs contain the frequencies of the source signals and is independent of each other, so the separation

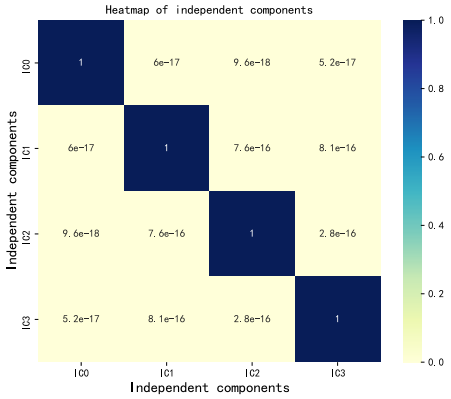

FIGURE 17. Heatmap of EMR signals of the four generators.

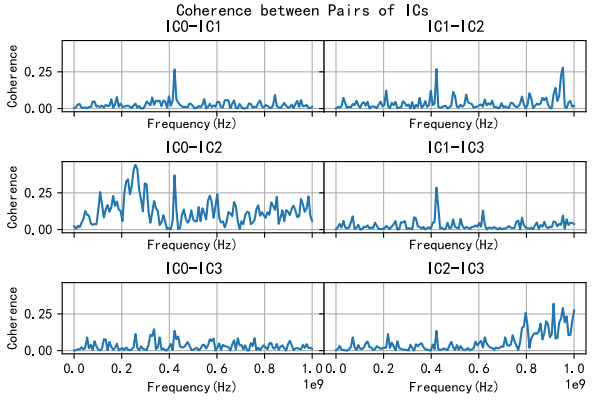

FIGURE 18. Coherence between pairs of ICs.

results can be proved to be correct. So far, this paper has realized the goal of synchronously separating electromagnetic radiation source signals from observation signals of different channels. Considering that the number of observation channels (3) is less than the number of source signals (4), this proves that our proposed algorithm can solve the problem of underdetermined blind source separation in complex field test environment. It is of great significance to accurately separate the source signals of electromagnetic radiation equipment from complex observation signals in the field environment for equipment fault diagnosis, electromagnetic compatibility test and monitoring of equipment operation status.

V. CONCLUSION

In this work, a method for synchronous multichannel EMR signal BSS was proposed to resolve the problems of shipboard EMR testing, i.e., high noise levels, mode mixing, and indeterminacy. As shipboard EMR signals are non-stationary and contain high levels of noise interference, MEMD was used in combination with ICA to separate these signals, while kurtosis was used as the criterion for IMF selection. Simulations and actual ship-based validations were performed to verify the efficacy of the proposed MEMD-ICA algorithm. The experimental results demonstrate that this algorithm is not affected by the mode mixing problems associated with MEMD decomposition and can perform BSS in the presence of strong noise interference. The proposed algorithm has high practical value as it is suitable for EMR testing in large equipment systems like ships, aircraft, spacecraft and national defense systems. However, there are certain limitations in the implementation of this algorithm. Since a large amount of EMR signal data was collected during the shipboard measurements, the MEMD-ICA algorithm required a long computational time. In our future work, we will further optimize the MEMD-ICA algorithm to enable its use in real-time shipboard EMR testing.

REFERENCES

[1] L. Sheng, W. Bangmin, and Z. Lanyong, "Intelligent adaptive filtering algorithm for electromagnetic-radiation field testing," *IEEE Trans. Electromagn. Compat.*, vol. 59, no. 6, pp. 1765–1780, Dec. 2017.

[2] Z.-H. Lu, L. Ding, X.-H. Lin, and M.-T. Lin, "An innovative virtual chamber measurement method based on spatial domain cancellation technique for radiation emission *in situ* test," *IEEE Trans. Electromagn. Compat.*, vol. 59, no. 2, pp. 342–351, Apr. 2017.

[3] B. Mijović, M. De Vos, I. Gligorijević, J. Taelman, and S. Van Huffel, "Source separation from single-channel recordings by combining empirical-mode decomposition and independent component analysis," *IEEE Trans. Biomed. Eng.*, vol. 57, no. 9, pp. 2188–2196, Sep. 2010.

[4] N. Mammone, F. La Foresta, and F. C. Morabito, "Automatic artifact rejection from multichannel scalp EEG by wavelet ICA," *IEEE Sensors J.*, vol. 12, no. 3, pp. 533–542, Mar. 2012.

[5] R. Mahajan and B. I. Morshed, "Unsupervised eye blink artifact denoising of EEG data with modified multiscale sample entropy, kurtosis, and wavelet-ICA," *IEEE J. Biomed. Health Informat.*, vol. 19, no. 1, pp. 158–165, Jan. 2015.

[6] S.-C. Ng and P. Raveendran, "Enhanced μ rhythm extraction using blind source separation and wavelet transform," *IEEE Trans. Biomed. Eng.*, vol. 56, no. 8, pp. 2024–2034, Aug. 2009.

[7] P. Lei, M. Chen, and J. Wang, "Speech enhancement for in-vehicle voice control systems using wavelet analysis and blind source separation," *IET Intell. Transp. Syst.*, vol. 13, no. 4, pp. 693–702, Apr. 2019.

[8] M. E. Davies and C. J. James, "Source separation using single channel ICA," *Signal Process.*, vol. 87, no. 8, pp. 1819–1832, Aug. 2007.

[9] C. Y. Sai, N. Mokhtar, H. Arof, P. Cumming, and M. Iwahashi, "Automated classification and removal of EEG artifacts with SVM and wavelet-ICA," *IEEE J. Biomed. Health Informat.*, vol. 22, no. 3, pp. 664–670, May 2018.

[10] M. A. Azpurua, M. Pous, and F. Silva, "Decomposition of electromagnetic interferences in the time-domain," *IEEE Trans. Electromagn. Compat.*, vol. 58, no. 2, pp. 385–392, Apr. 2016.

[11] K. P. Paradeshi, R. Scholar, and U. D. Kolekar, "Removal of ocular artifacts from multichannel EEG signal using wavelet enhanced ICA," in *Proc. Int. Conf. Energy, Commun., Data Anal. Soft Comput. (ICECDS)*, Aug. 2017, pp. 383–387.

[12] G. Wang, C. Teng, K. Li, Z. Zhang, and X. Yan, "The removal of EOG artifacts from EEG signals using independent component analysis and multivariate empirical mode decomposition," *IEEE J. Biomed. Health Informat.*, vol. 20, no. 5, pp. 1301–1308, Sep. 2016.

[13] M. H. Soomro, N. Badruddin, M. Z. Yusoff, and A. S. Malik, "A method for automatic removal of eye blink artifacts from EEG based on EMD-ICA," in *Proc. IEEE 9th Int. Colloq. Signal Process. Appl.*, Mar. 2013, pp. 129–134.

[14] M. Žvokelj, S. Zupan, and I. Prebil, "EEMD-based multiscale ICA method for slewing bearing fault detection and diagnosis," *J. Sound Vib.*, vol. 370, pp. 394–423, May 2016. [Online]. Available: http://www.sciencedirect.com/science/article/pii/S0022460X1600095X

[15] Y. Lei, J. Lin, Z. He, and M. J. Zuo, "A review on empirical mode decomposition in fault diagnosis of rotating machinery," *Mech. Syst. Signal Process.*, vol. 35, nos. 1–2, pp. 108–126, Feb. 2013. [Online]. Available: http://www.sciencedirect.com/science/article/pii/S0888327012003731

[16] Y. Yu, L. Congming, W. Tingyu, and Z. Xing, "Fault diagnosis and classification for bearing based on EMD-ICA," in *Proc. Int. Conf. Electron. Mech. Eng. Inf. Technol.*, vol. 5, Aug. 2011, pp. 2715–2718.

[17] K. Zeng, D. Chen, G. Ouyang, L. Wang, X. Liu, and X. Li, "An EEMD-ICA approach to enhancing artifact rejection for noisy multivariate neural data," *IEEE Trans. Neural Syst. Rehabil. Eng.*, vol. 24, no. 6, pp. 630–638, Jun. 2016.

[18] D. P. Mandic, N. U. Rehman, Z. Wu, and N. E. Huang, "Empirical mode decomposition-based time-frequency analysis of multivariate signals: The power of adaptive data analysis," *IEEE Signal Process. Mag.*, vol. 30, no. 6, pp. 74–86, Nov. 2013.
[19] X. Lang, Q. Zheng, Z. Zhang, S. Lu, L. Xie, A. Horch, and H. Su, "Fast multivariate empirical mode decomposition," *IEEE Access*, vol. 6, pp. 65521–65538, 2018.
[20] M. Hu and H. Liang, "Intrinsic mode entropy based on multivariate empirical mode decomposition and its application to neural data analysis," *Cognit. Neurodyn.*, vol. 5, no. 3, pp. 277–284, Sep. 2011.
[21] C. Park, D. Looney, N. U. Rehman, A. Ahrabian, and D. P. Mandic, "Classification of motor imagery BCI using multivariate empirical mode decomposition," *IEEE Trans. Neural Syst. Rehabil. Eng.*, vol. 21, no. 1, pp. 10–22, Jan. 2013.
[22] Y. Lv, R. Yuan, and G. Song, "Multivariate empirical mode decomposition and its application to fault diagnosis of rolling bearing," *Mech. Syst. Signal Process.*, vol. 81, pp. 219–234, Dec. 2016. [Online]. Available: http://www.sciencedirect.com/science/article/pii/S0888327016300048
[23] G. R. Naik, S. E. Selvan, and H. T. Nguyen, "Single-channel EMG classification with ensemble-empirical-mode-decomposition-based ICA for diagnosing neuromuscular disorders," *IEEE Trans. Neural Syst. Rehabil. Eng.*, vol. 24, no. 7, pp. 734–743, Jul. 2016.
[24] X.-L. Li and T. Adali, "Independent component analysis by entropy bound minimization," *IEEE Trans. Signal Process.*, vol. 58, no. 10, pp. 5151–5164, Oct. 2010.

SHENG LIU was born in 1957. He received the B.E. degree in industrial automation from the Harbin University of Civil Engineering and Architecture, in February 1982, and the master's and Ph.D. degrees in theory and control engineering from Harbin Engineering University, in March 1987 and March 2000, respectively.

He is currently a Professor with Harbin Engineering University. His current research interests include electromagnetic compatibility prediction and measurement, the optimization estimation and control of random systems, robust control, and ship control systems.

BANGMIN WANG received the B.Sc. degree from Harbin Engineering University in 2014, where he is currently pursuing the Ph.D. degree in electromagnetic compatibility prediction and measurement, and electromagnetic compatibility signal processing.

LANYONG ZHANG (Member, IEEE) received the Ph.D. degree in theory and control engineering from Harbin Engineering University, in 2011. His current research interests include the fast transient analysis and the modeling of field-excited multiconductor networks, power-line carrier propagation, electromagnetic field interference from overhead multiconductor lines, and electromagnetic interaction with advanced composite materials. He received the Excellent Graduate Award from the same university in August 2009.